Supplement of Atmos. Chem. Phys., 22, 14421–14439, 2022
https://doi.org/10.5194/acp-22-14421-2022-supplement

Atmospheric Chemistry and Physics
Open Access
EGU

Supplement of

Composition and mixing state of Arctic aerosol and cloud residual particles from long-term single-particle observations at Zeppelin Observatory, Svalbard

Kouji Adachi et al.

Correspondence to: Kouji Adachi (adachik@mri-jma.go.jp)

Possible nitrate contribution to sea salt particles

Previous studies (Chi et al., 2015; Geng et al., 2010) have shown that aged sea salt particles from the sites at Ny-Ålesund during the summer reacted with sulfate, nitrate, or both. They found significant amounts of nitrate with the sea salt particles, whereas in our study, the sea salt reactions mostly occurred with sulfates. A possible reason for the lack of nitrate in our samples is that our collected samples consist of smaller particles than those in previous studies. Our sample sizes were 0.3–1.3 μm in area equivalent diameters or 0.1–0.7 μm in aerodynamic diameters, whereas other studies used 0.7–13 μm in area equivalent diameters (Chi et al., 2015) and 0.5–8.0 μm in aerodynamic diameters (Geng et al., 2010). Because of evaporative losses of nitrate (Zhang and McMurry, 1992; Chow et al., 2005), the particle size used in this study may have been too small to retain nitrate on the surface. Differences in sampling altitude (mountain sites vs. ground-level sites) may also affect the occurrence of nitrates, as nitrate concentrations have been reported to be much lower than those of sulfate at Zeppelin Observatory (Karl et al., 2019).

Iodine-bearing particles

Iodine oxides are important in the Arctic because they accelerate new particle formation (Baccarini et al., 2020; Willis et al., 2018). Iodine is also known to be released from marine sources and reacts with sea salts through halogen chemistry in the atmosphere (Saiz-Lopez et al., 2012). We detected iodine-bearing particles in eight samples collected on two separate days (September 19 and October 9, 2017) from ambient aerosol and cloud residual samples (Fig. S3). Of these samples, iodine-bearing particles (iodine > 2 wt%) were heterogeneously present in the measured particles, as indicated by elemental mapping images. In our samples, 78% of iodine-bearing particles were detected in the sea salts.

References

Baccarini, A., Karlsson, L., Dommen, J., Duplessis, P., Vullers, J., Brooks, I. M., Saiz-Lopez, A., Salter, M., Tjernstrom, M., Baltensperger, U., Zieger, P., and Schmale, J.: Frequent new particle formation over the high Arctic pack ice by enhanced iodine emissions, *Nat. Commun.*, **11**, 4924, 10.1038/s41467-020-18551-0, 2020.

Chi, J. W., Li, W. J., Zhang, D. Z., Zhang, J. C., Lin, Y. T., Shen, X. J., Sun, J. Y., Chen, J. M., Zhang, X. Y., Zhang, Y. M., and Wang, W. X.: Sea salt aerosols as a reactive surface for inorganic and organic acidic gases in the Arctic troposphere, *Atmos. Chem. Phys.*, **15**, 11341-11353, 10.5194/acp-15-11341-2015, 2015.

Chow, J. C., Watson, J. G., Lowenthal, D. H., and Magliano, K. L.: Loss of PM2.5 nitrate from filter samples in central California, *J. Air Waste Manag. Assoc.*, **55**, 1158-1168, 10.1080/10473289.2005.10464704, 2005.

Geng, H., Ryu, J., Jung, H.-J., Chung, H., Ahn, K.-H., and Ro, C.-U.: Single-particle characterization of summertime Arctic aerosols collected at Ny-Ålesund, Svalbard, *Environ. Sci. Technol.*, **44**, 2348-2353, 10.1021/es903268j, 2010.

Karl, M., Leck, C., Mashayekhy Rad, F., Bäcklund, A., Lopez-Aparicio, S., and Heintzenberg, J.: New insights in sources of the sub-micrometre aerosol at Mt. Zeppelin observatory (Spitsbergen) in the year 2015, *Tellus B*, **71**, 1613143, 10.1080/16000889.2019.1613143, 2019.

Saiz-Lopez, A., Plane, J. M., Baker, A. R., Carpenter, L. J., von Glasow, R., Martin, J. C., McFiggans, G., and Saunders, R. W.: Atmospheric chemistry of iodine, *Chem. Rev.*, **112**, 1773-1804, 10.1021/cr200029u, 2012.

Willis, M. D., Leaitch, W. R., and Abbatt, J. P. D.: Processes controlling the composition and abundance of arctic aerosol, *Rev. Geophys.*, **56**, 621-671, 10.1029/2018rg000602, 2018.

Zhang, X., and McMurry, P. H.: Evaporative losses of fine particulate nitrates during sampling, *Atmos. Environ.*, **26**, 3305-3312, https://doi.org/10.1016/0960-1686(92)90347-N, 1992.

Supplemental figures

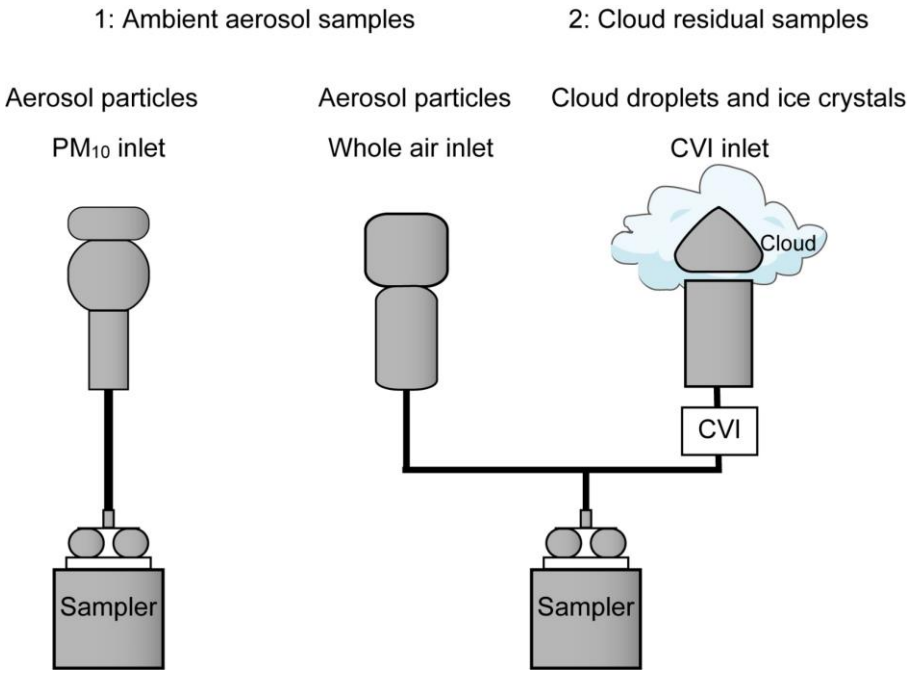

Figure S1. Schematic illustration of inlets and samplers used in this study. Samples from both PM_{10} and whole-air inlets were classified into ambient aerosol samples. Samples from the CVI inlet were classified into cloud residual samples.

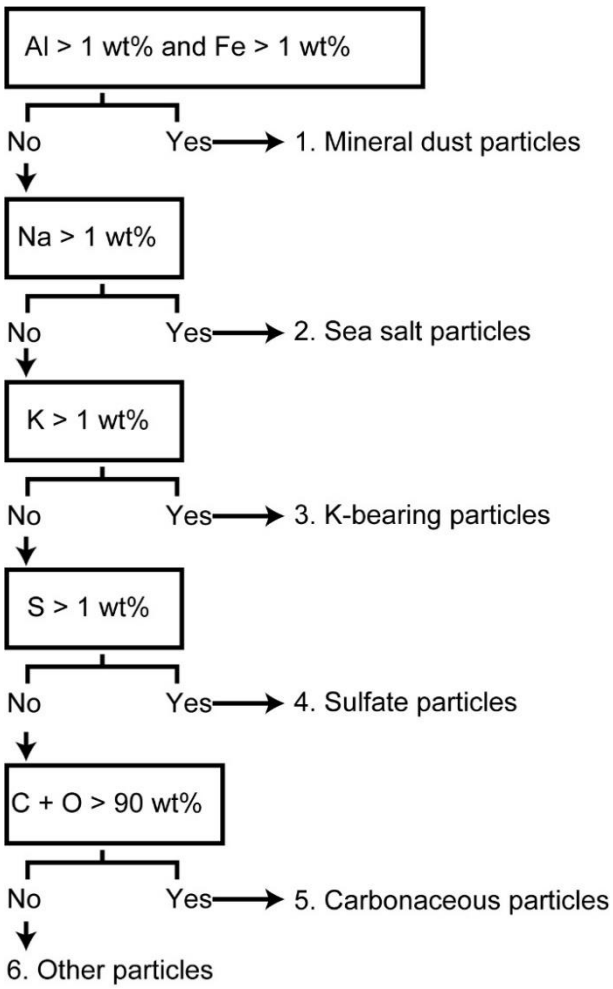

Figure S2. Flow chart of particle classification based on composition measured using STEM-EDS.

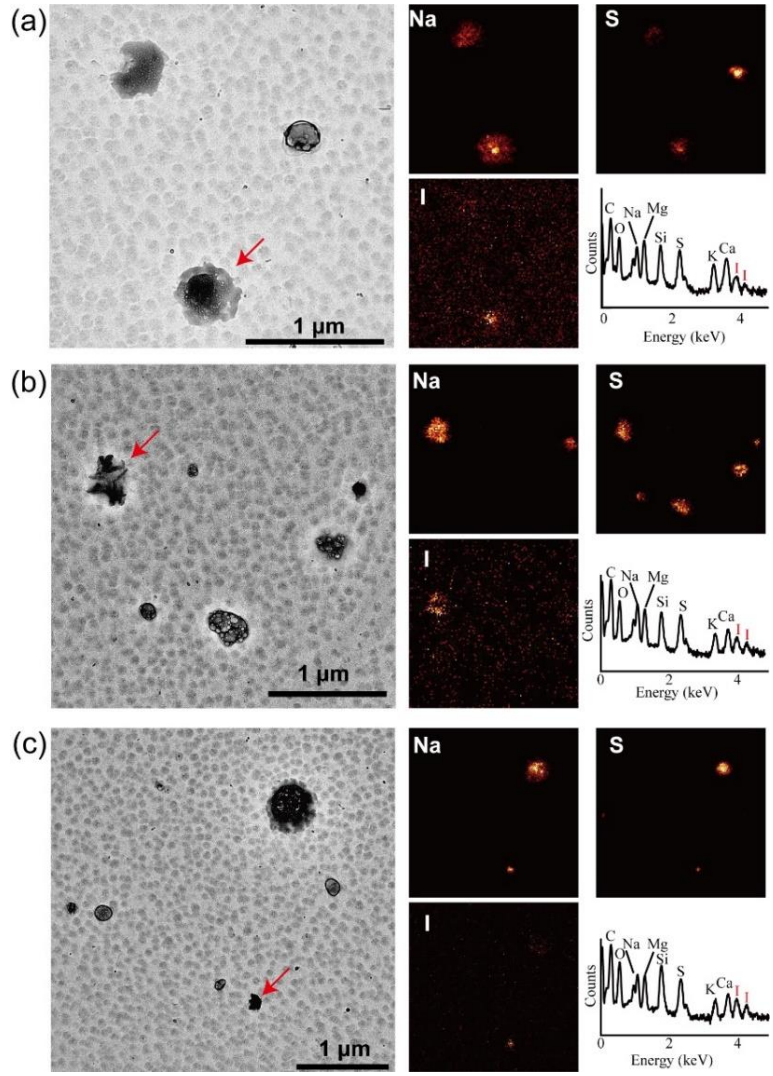

Figure S3. Examples of TEM and elemental mapping images and EDS spectra of iodine(I)-bearing particles are indicated by red arrows (a–c). These particles were derived from the ambient aerosol samples collected on September 19, 2017 (08:36). The EDS spectra of iodine-bearing particles show peaks at L_{α} 3.9 keV and $L_{\beta 1}$ 4.2 keV. Iodine coexists with Na, S, Mg, Si, K, and Ca.

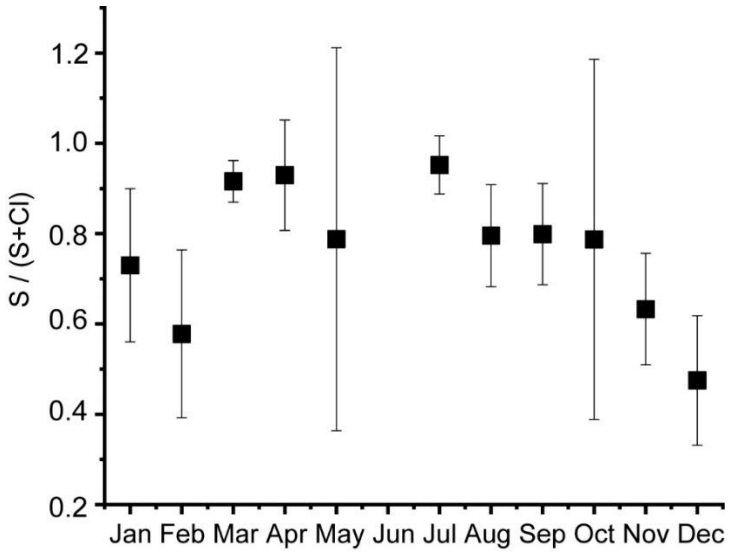

Figure S4. Monthly average values of S/(S + Cl) (calculated from their wt% values) in sea salt particles from ambient aerosol samples. Error bars indicate a confidential interval of 95%. When sea salt particles react with sulfates, this ratio increases toward 1. The numbers of TEM samples are 14, 3, 59, 4, 3, 0, 14, 32, 24, 3, 22, and 16 from January to December, respectively.

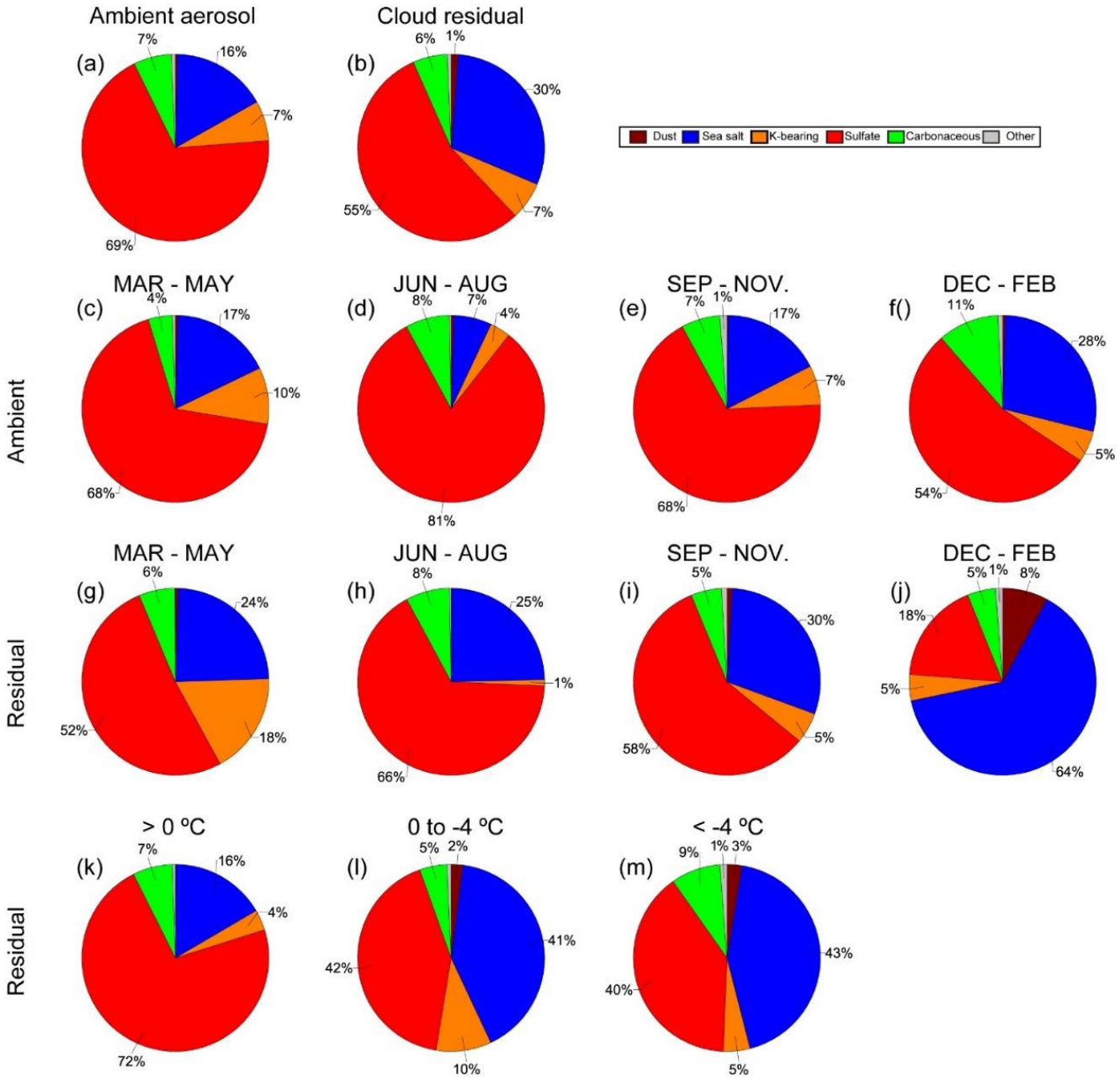

Figure S5. Number fractions of aerosol particle types for ambient aerosol and cloud residual samples. These numbers and sample classifications are the same as those in Figs. 7-8 and 10. All (a) ambient aerosol and (b) cloud residual samples; ambient aerosol samples (c) from March to May, (d) from June to August, (e) from September to November, and (f) from December to February; cloud residual samples (g) from March to May, (h) from June to August, (i) from September to November, and (j) from December to February. Cloud residual samples collected at (k) >0°C, (l) 0°C to −4°C, and (m) <−4°C. Only percentages ≥1 are shown as numbers in each diagram.

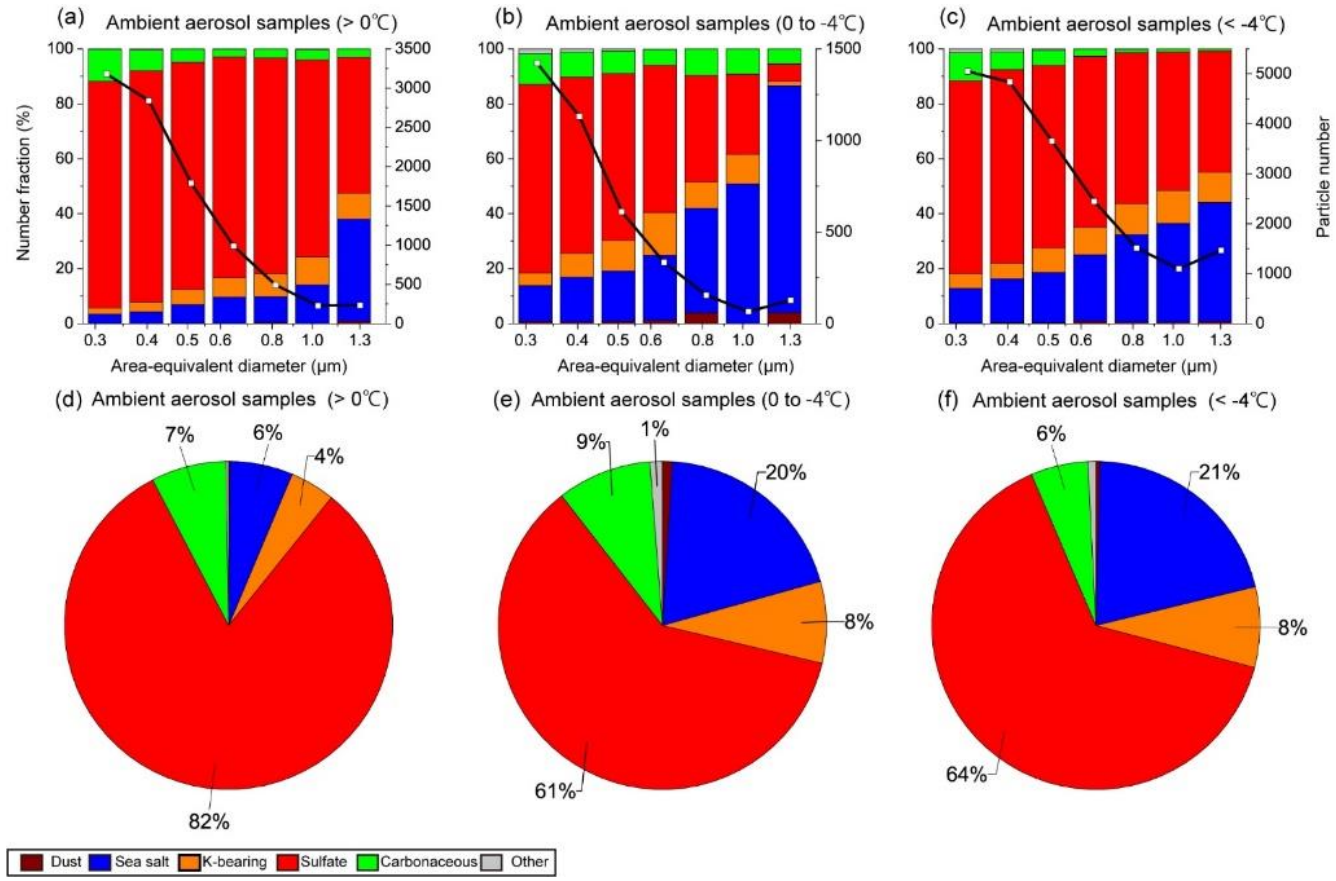

Figure S6. Size-dependent number fractions of aerosol types and the number distributions for ambient aerosol samples collected at (a) >0°C, (b) 0°C to −4°C, and (c) <−4°C. N = (a) 9747, (b) 3845, and (c) 20,060. (d) to (f): Same samples as (a) to (c) but representing their abundances for all size ranges.

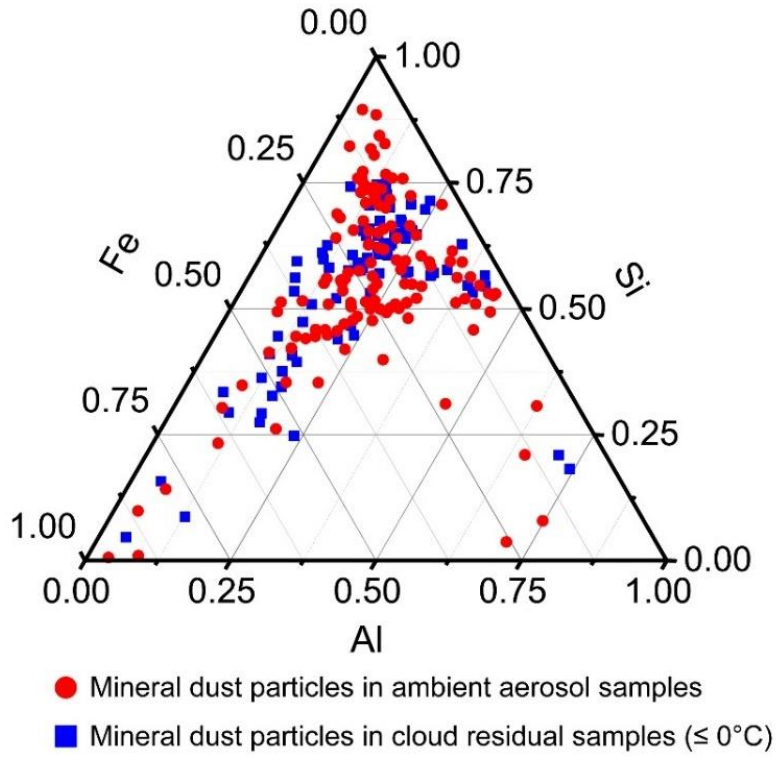

Figure S7. Ternary plot of Al, Si, and Fe (relative values in wt%) for individual mineral dust particles in ambient aerosol samples (all temperatures, red circles) and cloud residual samples (≤ 0°C, blue squares). N = 125 and 82 for mineral dust particles from ambient aerosol samples and cloud residual samples (≤ 0°C), respectively.

Table S1. Average size (area equivalent diameter) and composition of mineral dust particles, sea salt particles, K-bearing particles, sulfate particles, carbonaceous particles, and other particles.

Aerosol type	Area-equivalent diameter (μm)	C (wt%)	O (wt%)	Na (wt%)	Mg (wt%)	Al (wt%)	Si (wt%)	S (wt%)	Cl (wt%)	K (wt%)	Ca (wt%)	Cr (wt%)	Mn (wt%)	Fe (wt%)	Minor	N
Mineral dust	0.56 ± 0.05	39 ± 2.5	25 ± 1.1	2.2 ± 0.4	1.8 ± 0.2	4.4 ± 0.5	10.7 ± 0.9	5.4 ± 0.7	1.5 ± 0.5	2.0 ± 0.3	1.3 ± 0.3	0.34 ± 0.4	0.3 ± 0.3	5.6 ± 1	P, Ti, Ni, Zn	213
Sea salt	0.57 ± 0.01	52 ± 0.5	16 ± 0.2	8.5 ± 0.2	1.6 ± 0.1	< 0.1	3.6 ± 0.1	8.9 ± 0.2	6.4 ± 0.3	1.2 ± 0.1	0.7 ± 0.02	< 0.1	< 0.1	0.5 ± 0.1	Ni, Zn, I	7697
K-bearing	0.53 ± 0.01	72 ± 0.4	12 ± 0.2	0.3 ± 0.01	< 0.1	< 0.1	4.4 ± 0.1	7.5 ± 0.2	< 0.1	2.8 ± 0.1	< 0.1	< 0.1	< 0.1	0.6 ± 0.1	N, I	2796
Sulfate	0.43 ± 0.01	78 ± 0.1	10 ± 0.1	0.2 ± 0	< 0.1	< 0.1	5.2 ± 0.1	5.2 ± 0.1	< 0.1	0.1 ± 0.01	< 0.1	< 0.1	< 0.1	0.6 ± 0.1	N, I	27173
Carbonaceous	0.37 ± 0.01	89 ± 0.1	7 ± 0.1	0.1 ± 0.01	< 0.1	< 0.1	3.2 ± 0.1	0.6 ± 0.1	< 0.1	< 0.1	< 0.1	< 0.1	< 0.1	0.4 ± 0.1		2634
Others	0.34 ± 0.01	70 ± 1.8	14 ± 0.7	0.2 ± 0.02	0.2 ± 0.1	< 0.1	12.1 ± 0.8	0.7 ± 0.1	0.1 ± 0.1	< 0.1	0.3 ± 0.2	< 0.1	< 0.1	1.9 ± 1.0	Ti, Zn, I	277

95% confidence interval values are shown. Minor elements are those between 0.1 and 0.2 wt%. Less than 0.1% by weight is indicated as <0.1. Carbon can also be derived from the substrate. N: number of particles detected.

Table S2. Averaged temperature, relative humidity, and wind speed during the whole sampling period. The ranges show standard deviations. The averaged values were obtained from hourly data.

Month	Seasons	Temperature	Relative humidity	Wind speed
		℃	%	m/S
DEC-FEB	Spring	-10 ± 7	77 ± 17	4 ± 3
MAR-MAY	Summer	2 ± 4	86 ± 13	3 ± 2
JUN-AUG	Fall	-4 ± 5	82 ± 13	4 ± 3
SEP-NOV	Winter	-11 ± 6	74 ± 16	5 ± 3